Published in final edited form as:
Anal Chem. 2013 March 5; 85(5): 2760–2769. doi:10.1021/ac303273z.

Carbohydrate Structure Characterization by Tandem Ion Mobility Mass Spectrometry (IMMS)[2]

Hongli Li[1], **Brad Bendiak**[2], **William F. Siems**[1], **David R. Gang**[3], and **Herbert H. Hill Jr.**[1,*]

[1]Department of Chemistry, Washington State University, Pullman, Washington, US

[2]Department of Cell and Developmental Biology, Program in Structural Biology and Biophysics, University of Colorado, Health Sciences Center, Anschutz Medical Campus, Aurora, Colorado, USA

[3]Institute of Biological Chemistry, Washington State University, Pullman, Washington, US

Abstract

A high resolution ion mobility spectrometer was interfaced to a Synapt G2 high definition mass spectrometer (HDMS) to produce IMMS-IMMS analysis. The hybrid instrument contained an electro-spray ionization source, two ion gates, an ambient pressure linear ion mobility drift tube, a quadrupole mass filter, a traveling wave ion mobility spectrometer (TWIMS) and a time of flight mass spectrometer. The dual gate drift tube ion mobility spectrometer (DTIMS) could be used to acquire traditional IMS spectra, but also could selectively transfer specific mobility selected precursor ions to the Synapt G2 HDMS for mass filtration (quadrupole). The mobility and mass selected ions could then be introduced into a collision cell for fragmentation followed by mobility separation of the fragment ions with the traveling wave ion mobility spectrometer. These mobility separated fragment ions are finally mass analyzed using a time-of-flight mass spectrometer. This results in an IMMS-IMMS analysis and provides a method to evaluate the isomeric heterogeneity of precursor ions by both DTIMS and TWIMS, to acquire a mobility-selected and mass-filtered fragmentation pattern and to additionally obtain traveling wave ion mobility spectra of the corresponding product ions. This new IMMS[2] instrument enables the structural diversity of carbohydrates to be studied in greater detail. The physical separation of isomeric oligosaccharide mixtures was achieved by both DTIMS and TWIMS, with DTIMS demonstrating higher resolving power (70~80) than TWIMS (30~40). Mobility selected MS/MS spectra were obtained, and TWIMS evaluation of product ions showed that isomeric forms of fragment ions existed for identical *m/z* values.

Introduction

Since the first discussion of ion mobility spectrometry (IMS) or plasma chromatography in the 1970's,[1–4] IMS has been applied as an analytical separation and detection tool for explosives,[5–8] drugs,[9–11] chemical warfare reagents[12–14] and biological compounds.[15–17] IMS is a unique gas phase ion separation technique based on the ion's collision cross section (Ω),[18,19] which makes it an ideal candidate for differentiation of isomers having identical *m/z* values but different structures or configurations. When coupled with mass spectrometry (MS),[20–23] IMS becomes a powerful analytical tool called ion mobility mass spectrometry (IMMS)[24] in which the mass-to-size ratio (m/Ω) provides a measure of an ion's cross section m/Å^2 density. The benefits of IMMS separation include increasing the peak capacity of a

*To whom Correspondence should be addressed. Herbert H. Hill, Jr., Department of Chemistry, Washington State University, Pullman, WA 99164, hhhill@wsu.edu, Tel 509-335-5648.

mass spectrometer, separating compounds with the same *m/z* values,[25] reducing chemical and random noise,[26] measuring Ω/z values,[27] offering class identification by mobility-mass correlation lines[28–30] and charge state separation.[31] IMMS has proved particularly useful for the separation and identification of biomolecules in complex mixtures such as those encountered in metabolomics,[26, 30, 32, 33] glycomics[31, 34, 35] and proteomics.[36–38] Conventionally, IMMS instruments utilize IMS either at atmospheric pressure or reduced pressure as a separator for gas phase ions followed by a mass analyzer to provide *m/z* information. Recently, a traveling wave IMMS,[39–41] the Synapt G2 high definition mass spectrometry (HDMS),[42,43] was developed and has been widely used.[44–49] It is a hybrid quadrupole/ion mobility separator/orthogonal-TOF instrument. The design, electric field homogeneity and pressure are different from traditional drift tube IMS. Moreover, an additional trap and transfer cells were installed in the front and after the traveling wave ion mobility spectrometer (TWIMS) and could be used to fragment ions before and/or after traveling wave mobility separations.

The primary structures of carbohydrates are extremely complicated compared to nucleic acids and proteins, normally existing in numerous isomeric forms[50–52] due to differences in the stereochemistry of their monosaccharides, branching of the structures and alternate linkage locations between sugar units. It has been shown that isomeric oligosaccharide species, either simple standards or mixtures prepared from biological sources, can be resolved on the mobility scale.[25, 31, 34, 53–55] By installing a second gate[23, 55, 56] or selection gate[57] in IMS and connecting the instrument to a tandem mass spectrometer, mobility-selected fragmentation spectra can be collected to provide evidence for differences in structures between mobility-separated isomeric carbohydrate precursor ions. Compared to LC, the most commonly employed separation method, IMS provides advantages of speed (μs or ms scale) and sensitivity, with comparable or higher resolving power for the separation of isomers. Currently, although a number of studies have focused on characterization of isomeric carbohydrate precursor ions employing IMS, structural variation of isomeric product ions has not been extensively investigated.[58] Clemmer et al.[58] showed the mobility of product ions of simple oligosaccharides by fragmenting precursor ions with high injection energy prior to IMS. In the Synapt G2 instrument, a trap cell is installed in front of a TWIMS, which enables the isomeric heterogeneity of product ions to be evaluated. However, determining the mobilities of both precursor and product ions, where product ions are derived from precursor ions within a specific mobility window, is not currently feasible for isomeric carbohydrate mixtures. Consequently, the mobility spectra of product ions generated from a mixture of isomeric precursor ions results in ambiguous precursor-product ion relationships. It is impossible to assign the mobility peaks of product ions to specific precursor ions in these cases.

In this study, we describe a new ion mobility mass spectrometry instrument, a dual gate drift tube IMS (DTIMS) interfaced to a Synapt G2 HDMS, which provides a novel analytical approach of IMMS-IMMS. It is capable of carrying out an additional MS function compared to the IMS-IMS instrument reported previously.[62] This is also the first instrument that incorporates DTIMS, TWIMS, mass selection, mobility selection and tandem MS together. Mixtures of isomeric oligosaccharides were used to evaluate multiple capabilities of this hybrid instrument. Results include mobility separation of isomeric mixtures of precursor ions using both DTIMS and TWIMS, mobility-selected tandem spectra and traveling wave ion mobility evaluation of product ions derived from mobility and mass selected precursor ions.

Experimental Section

Chemicals and solvents

NaCl, D-Gal-α-1–4-D-Gal (4α-galactobiose), D-Glc-β-1–6-D-Glc (gentiobiose), the trisaccharides raffinose and maltotriose, and the pentasaccharides cellopentaose and maltopentaose were purchased from Sigma Chemical Co., St. Louis, Missouri. The pentasaccharide [D-Man-α-1–6-[D-Man-α-1–3]-D-Man-α-1–6]-[D-Man-α-1–3]-D-Man (branched $(Man)_5$ is used in the following text) was purchased from V-labs, Covington, Louisiana. LC-MS grade solvents of methanol and water were purchased from Thermo Fisher Scientific Inc.. Disaccharide-alditols D-Gal-α-1–4-D-Gal-ol and D-Glc-β-1–6-D-Glc-ol were prepared from 4α-galactobiose and gentiobiose (See supporting information for the reduction method, similar to a previously published procedure[63]).

Sample preparation

200 μM stock solutions of disaccharide-alditols with 200 μM NaCl in each sample were initially prepared using electro-spray (ESI) solvent (50:50 v:v methanol: water) and were diluted in 1:1 ESI solvent for individual analysis (100 μM each). They were mixed unequally resulting in a mixture of 100 μM D-Gal-α-1–4-D-Gal-ol and 50 μM D-Glc-β-1–6-D-Glc-ol. Raffinose and maltotriose were prepared in the same way; raffinose at 50 μM, maltotriose at 100 μM in the mixture. Unequal concentrations of samples in the mixture were used to decrease ion suppression effects. 300 μM stock solutions of pentasaccharides with 300 μM NaCl in each sample were prepared and were mixed in equal volumes for mixture analysis (100 μM each). They were then diluted 1:2 in ESI solvent for separate analyses of individual compounds (100 μM each).

Electrospray ionization (ESI)

The details of the construction of the lab-built ESI source are included in the supporting information.

Dual gate drift tube ion mobility spectrometer (DTIMS)

Two Bradbury-Nielson ion gates separated the IMS tube into a desolvation region (7.5 cm length), drift region (21.0 cm length) and post drift region (1.0 cm length). Nitrogen was used as the drift gas at a flow rate of 2 L/min and the tube was maintained at 180°C. Voltages at the first ring, first ion gate, second ion gate and last ring of IMS tube were 10.0 KV, 9.01 KV, 743 V and 427 V, respectively, resulting in a homogeneous electric field of 394 V/cm. The control software and operations of the dual gate IMS system were the same as described in previous publications,[23, 56, 55] except that the software was updated with the 2009 version of Labview (National Instruments, Austin, TX). Briefly, there are two operation modes: dual gate scanning (DGS) which determines the drift time of an ion by a series of successive stepped ion gate pulsing experiments and selected mobility monitoring (SMM) which allows ions of specific drift time window widths to be transferred to the mass analyzer. For the results shown in this study, the parameters used for the DGS mode were as follows: the gate pulse widths of both ion gates were 0.3 ms, the step resolution (the increment by which the second gate delay was sequentially increased) was at 0.1 ms, pulses/step (number of ion gate pulses before the 2nd gate is moved to the next delay) was set at 300, and the scan window was normally within 3 or 4 ms as defined from the second gate delay. For the SMM mode, the first ion gate was kept at 0.3 ms, and the second gate was open for a certain drift time range (specified for different compounds) to select the target analyte. The pulsing of the first ion gate of the DTIMS was synchronized with the data acquisition of the MS in both modes.

Dual gate DTIMS interfaced to Synapt G2 HDMS

The Synapt G2 HDMS instrument has been described elsewhere.[39–43] The TWIMS is used under reduced pressure and employs traveling wave ion guide technology with a non-uniform electric field. The overall schematics of the ESI, ambient pressure, dual gate DTIMS, Synapt G2 HDMS instrument and the detailed interface connection (inset) are displayed in Figure 1. To make the connection, the original sample cone was replaced with a modified sample cone which is almost identical to the original one except that an extended threads section (i. d. 1/8″) was added to the orifice (the pictures of original and modified sample cones are shown in Figure S-1 in supporting information). The end of the DTIMS tube was sealed with a metal plate having an extended threaded orifice (i. d. 1/8″) in the center and was electrically isolated from the last ring of the DTIMS by ceramic rings. A hollow stainless steel tube (o. d. 1/8″, i. d. 1/24″) having a 90 degree bend with unequal lengths on either side of the bend (4 cm and 2 cm), was used to connect the orifice on the metal plate of the DTIMS with the modified sample cone on the Synapt G2. The voltages on the metal plate and 90 degree tube were the same to the voltage as applied on the sample cone which was −68 V when the Synapt G2 was in the TOF mode and 87 V when the Synapt G2 was in the mobility TOF mode (positive ion mode). The TWIMS was operated with 40 V wave height, 650 m/s wave velocity at a pressure of ~ 3.5 mbar. Nitrogen was used as the drift gas at a flow rate of 90 mL/min, He was introduced at 180 mL/min to the helium cell installed in front of the ion mobility separator. Argon was used in the trap and transfer cells at a flow rate of 2 mL/min. The trap release time was 200 μs, and the mobility separation delay after the trap release was enabled and set at 450 μs. Masslynx 4.1 (Waters Corporation, Milford, MA, USA) was used to collect and process the data.

Operation modes of the hybrid DTIMS-Synapt G2 instrument

The hybrid DTIMS-Synapt G2 instrument was mainly operated in three modes in this study: (1) with both gates open, the DTIMS serves as an ion transmission device, and the system is in essence a Synapt G2 HDMS only; different data can be collected including traveling wave ion mobility spectra of mixture and standards, the fragmentation spectra and traveling wave ion mobililty spectra of product ions acquired from the standard run individually. (2) with the dual gate IMS operating in the DGS mode and the Synapt G2 working only as a TOF mass analyzer, the system is an atmospheric pressure DTIMS-TOFMS, whereby traditional drift tube ion mobility spectra of mixture and standards can be obtained; (3) with the dual gate IMS operating in SMM mode, compounds within a selected drift time range on the DTIMS can be transferred to the Synapt G2 for further analysis including mass selection by the quadrupole, fragmentation in the trap cell and TWIMS evaluation of product ions, in sequential order. The mobility- and mass-selected fragmentation spectra and traveling wave ion mobility spectra for product ions derived from specific isomeric precursor saccharides from a mixture were obtained using this mode.

Results and Discussion

Disaccharide alditols: D-Gal-α-1-4-D-Gal-ol and D-Glc-β-1-6-D-Glc-ol

With both DTIMS and TWIMS incorporated into one system, it is convenient to compare the separation capabilities of the two types of IMS. The isomeric disaccharide-alditols D-Gal-α-1-4-D-Gal-ol and D-Glc-β-1-6-D-Glc-ol were first investigated. It should be noted that all the *m/z* values reported for oligosaccharides in this study were sodiated adducts in the positive ion mode. Reduction of several specific disaccharides was carried out because the reducing sugar of disaccharides can exist in two or more configurations (α and β pyranose or furanose forms). This can complicate drift profiles if the different configurations happen to separate, an outcome that can be obviated by reduction. Figures 2a and 2b show the mobility spectra of the disaccharide-alditol mixture by TWIMS and DTIMS, respectively.

The data was acquired for 2 mins using the TWIMS and for 4 mins using the DTIMS. It is apparent that DTIMS demonstrated higher resolving power and better resolution between isomers. According to the traditional definition of resolving power (R_p) which is drift time divided by the peak width at half maximum, the experimental R_p for DTIMS in this study was 75 ± 5 and the temporal R_p for TWIMS was ~20 which corresponds to a mobility resolution of ~40.[41] By comparing the spectra of the mixture (Figures 2a and 2b) with the overlaid corresponding individual spectra displayed in Figures 2c and 2d, D-Glc-β-1-6-D-Glc-ol (peak 2) had a slower mobility than D-Gal-α-1-4-D-Gal-ol (peak 1). A strong ion suppression effect was observed in the mixture, with D-Gal-α-1-4-D-Gal-ol (100 μM) detected at lower intensity than D-Glc-β-1-6-D-Glc-ol (50 μM). This may be due to charge competition between the neutral compounds and the sodium present in the ionization solution, resulting in a possible competition for sodium with different ionization capabilities in a mixture. As discussed by Wesdemiotis[59] and Bowers,[60] Na^+ ions tend to coordinate with oxygen sites in carbohydrates through multidentate interactions, which can distort the normal structures of the neutral molecules. This results in experimentally preferred conformations for Na^+ adducts of sugar stereoisomers with differences in their overall shapes. Hence, the separation of isomers in IMS results from both the structural differences and also the conformational changes induced by Na^+ complexation.

Once the drift times of the carbohydrates were determined, selected mobility mode experiments were conducted for 10 mins for all the samples in this study to acquire mobility selected MS/MS data and also TWIMS spectra of fragment ions. Figures 2e and 2f display the mobility selected fragmentation spectra for D-Gal-α-1-4-D-Gal-ol and D-Glc-β-1-6-D-Glc-ol respectively by transferring mobility peaks 1 and 2 (Figure 2b) to the trap cell of the Synapt G2 separately. The 2nd gate windows on the DTIMS of 24.5–25.2 ms and 25.5–26.5 ms were used, respectively. The corresponding structures and proposed fragmentation pathways of the isomers are shown on the right. A major product ion of *m/z* 205 that resulted from glycosidic cleavage of the precursor ion (*m/z* 367) was observed for both disaccharide-alditols, but in very different abundance. In mass spectrometry of sugars, cleavages at glycosidic linkages are common; sodium was highly preferentially adducted with the alditol of these compounds and dissociation at the glycosidic linkage is accompanied by proton transfer from the glycon via one of several proposed mechanisms.[64, 65] Even with a higher collision energy (CE) of 40V applied to D-Glc-β-1-6-D-Glc-ol compared to that of 35 V applied to D-Gal-α-1-4-D-Gal-ol, the intensity of *m/z* 205 was still lower for D-Glc-β-1-6-D-Glc-ol which makes the two spectra distinguishable. The subsequent traveling wave mobility of fragment *m/z* 205 was almost the same for the two disaccharide-alditols. Their TWIMS spectra as well as the fragmentation spectra acquired from individual standards are displayed in Figures S-2 and S-3 in the supporting information. It is worthy of note that the percent error for different mass ions observed in this study was ~ ±3%; product ion mobility profiles yielded reproducible product ion ratios using the same collision energy in the trap cell.

Isomeric trisaccharides: raffinose and maltotriose

Figures 3a and 3b display the mobility separation of a mixture of structural isomers of raffinose (D-Gal-α-1-6-D-Glc-β-1-2-D-Fru) and maltotriose (D-Glc-α-1-4-D-Glc-α-1-4-D-Glc) using TWIMS and DTIMS respectively. There was little or no separation in TWIMS but partial separation was observed in DTIMS labeled as peaks 1 and 2. Ion suppression was also evident with raffinose having higher ionization efficiency in the mixture even at comparatively lower concentration (50 μM) than maltiotriose (100 μM). In comparison with mobility profiles acquired from their individual standards (Figures 3c and 3d), raffinose drifted faster than maltotriose. In addition, another small mobility shoulder peak was observed for maltotriose in both TWIMS and DTIMS by expanding the intensity scale as

shown in the inserted windows of Figures 3c and 3d. Higher resolving power and resolution were again demonstrated using DTIMS. Raffinose is termed a non-reducing oligosaccharide as both the Glc and Fru sugar units are glycosidically linked to each other at their anomeric positions, which locks each of these sugars in a single cyclic configuration. However, maltotriose is a reducing trisaccharide (see structure at the bottom right of Figure 3) having an –OH group at the reducing end in either the α or β pyranose configuration or even the aldehyde open chain form, which can result in more than one isomeric form for the molecule as examined by IMS. Direct evidence of the ring opening of monosaccharide anions in the gas phase has been demonstrated by Brown et al. in 2011.[66] Therefore, different Na^+ complexed maltotriose ions could be formed with different collision cross-sectional areas and it is not unexpected to have more than one mobility peak detected. Figures 3e and3f are the corresponding MS/MS spectra for mobility peaks 1 and 2 in Figure 3b by selecting the compounds with drift time windows of 31–31.5 ms and 32–32.5 ms on DTIMS respectively and applying the same CE (53 V) in the trap cell of the Synapt G2. The structures and proposed fragmentation pathways for peak 1 which is raffinose and peak 2 which is maltotriose are shown on the right. Both compounds with precursor ions of *m/z* 527 gave rise to predominant product ions of *m/z* 365 and product ions of *m/z* 347 and 203 as well. However, more fragments were observed for maltotriose such as *m/z* 185, 305, 407, 467 and 509 where *m/z* 509, 347 and 185 were derived from the H_2O loss from product ions of *m/z* 527, 365 and 203. These differences in fragmentation spectra demonstrated that the compounds were isomers and provided evidence for the mobility-separated precursor ions within the mixture. Moreover, all the fragments were reproducible using individual standards and the relative abundance was consistent for all the major fragments as well (see Figure S-4 in supporting information).

All the ions that resulted from the collision induced dissociation (CID) in the trap portion of the Synapt G2 shown in Figures 3e and 3f were then evaluated by the TWIMS. Figures 4a and 4b are the TWIMS spectra of the product ions corresponding to selected peak 1 (raffinose) and peak 2 (maltotriose) from the mixture with the system operating in mode 3, respectively and the corresponding *m/z* values for the major resolved mobility peaks are indicated. The same spectra acquired by injecting raffinose and maltotriose standards under identical experimental conditions are shown in Figures 4c and d, which unambiguously reproduced the data acquired from mobility selection experiments (Figures 4a and 4b). It was observed that product ions with smaller *m/z* values were distributed with faster drift times. The drift time values for the most abundant product ion *m/z* 365 were 3.47 and 3.53 ms for raffinose and maltotriose respectively, and they were barely resolved. More mobility peaks were detected in Figure 4b which corresponded to other unique fragments of maltotriose as shown in Figure 3f. Mobility identities of product ions derived from individual mobility-selected precursor ions from a mixture of isomers were able to be measured for the first time. In addition, the overall mobility profiles of product ions were obviously different for dissociated raffinose and maltotriose which could serve as further identities to differentiate the isomeric compounds. It is important to note that a direct precursor-product relationship can be established for individual product ions at 3.47 and 4.83 ms, for the first isomer, raffinose and at 2.28, 2.98, 3.53, 4.34 and 5.05 ms, for the second isomer, maltotriose, with each product ion mobility having a measurable *m/z*. Moreover, as can be seen (Figure 4), each isomer yields a consistently reproducible profile of product ion ratios provided the collision energy in the trap cell is the same. This direct relationship is not possible to establish unambiguously from a mixture of isomeric precursor ions only selected by *m/z*, i.e. where a mixture of isomeric precursors are simultaneously dissociated using CID. This should provide a valuable tool for assessment of the complexity of isomeric precursor ion mixtures and for firmly establishing their specific sets of product ions.

Isomeric pentasaccharides: cellopentaose, maltopentaose and brancehed $(Man)_5$

To further demonstrate the capability of the hybrid IMS-Synapt G2, isomeric oligosaccharides of higher molecular weight were investigated: cellopentaose [D-Glc-α-1-4-(D-Glc-α-1-4)$_3$-D-Glc], maltopentaose [D-Glc-β-1-4-(D-Glc-β-1-4)$_3$-D-Glc] and branched $(Man)_5$. Cellopentaose and maltopentaose are both composed of five glucose monomers but one is in α-1-4 linkage and the other in β-1-4 linkage. The mixture of these three isomeric pentasaccharides was resolved into two partially separated peaks using TWIMS as shown in Figure 5a. Interestingly, they were separated into four mobility peaks on DTIMS as shown in Figure 5b where three abundant peaks were labeled as peaks 1, 2 and 3. The traveling wave ion mobility spectrum of the mixture was acquired for 3 mins, and the time taken to scan the 4 ms range of the mixture by dual gate DTIMS was ~8 mins. Figures 5c and 5d display the overlaid mobility spectra of the individual pentasaccharides using TWIMS and DTIMS respectively. It was observed that cellopentaose had the fastest mobility, branched $(Man)_5$ had the slowest mobility, and maltopentaose was in the middle. In addition, two peaks were observed for cellopentaose using DTIMS. All the compounds had essentially identical drift time values within the mixture as compared to running them individually and the relative elution order of the compounds was the same using both types of IMS. The three pentasaccharides presented here are all reducing oligosaccharides (see structures on the right of Figure 6), having a reducing monosaccharide that exists in solution in at least two predominant (α and β pyranose) configurations, as discussed earlier. The low abundant mobility peak of cellopentaose detected by DTIMS is therefore not surprising, which may denote the α/β or open chain configuration. The relatively low resolving power of TWIMS makes this corresponding peak undetectable. Even though only one mobility peak was observed for maltopentaose and branched $(Man)_5$, it is still possible that more than one reducing-end configuration could exist for them and the Ω differences may simply be small enough where they co-migrate as one peak.

Based on the drift time values determined, second gate drift time windows of 38–38.7 ms, 39.5–40.3 ms and 40.6–41.5 ms on the DTIMS were used. These correspond to mobility peaks 1, 2 and 3 as shown in Figure 5 and were used to acquire the mobility selected MS/MS spectra for cellopentaose, maltopentaose and branched $(Man)_5$, respectively, from the mixture with the hybrid instrument operating in mode 3. The spectra are displayed in Figures 6a, 6b and 6c, respectively. A trap CE of 80 V was used for all three peaks and the corresponding structures and fragmentation pathways are also included (Figure 6). Varying solely in their anomeric configurations, the major product ions observed for cellopentaose and maltopentaose were almost identical but were present in different abundance. Those include ions of *m/z* 689, 527, 365, and 203 that resulted from glycosidic bond cleavage, X type ions of *m/z* 731, 569, and 407 and A type ions of *m/z* 791, 629, 467, and 305 according to the nomenclature of Domon and Costello.[61] In addition, the loss of H_2O was also widely observed among product ions such as *m/z* 833 (H_2O loss from *m/z* 851), 671 (H_2O loss from *m/z* 689), 509 (H_2O loss from *m/z* 527) and 347 (H_2O loss from *m/z* 365). The *m/z* 509 product ion appeared as the base peak for cellopentaose, while *m/z* 347 was detected having the maximum intensity for maltopentaose. Moreover, the relative intensities of product ion pairs of *m/z* 509/527 and *m/z* 671/689 were different for the two isomers as shown in Figures 6a and b. Branched $(Man)_5$ dissociated to yield all the major product ions observed for cellopentaose and maltopentaose, but in a dramatically different intensity distribution having *m/z* 527 and 689 as major fragments. Moreover, three unique product ions of *m/z* 275, 437 and 599, which are derived from cross ring cleavage as proposed on the structure shown in Figure 6 were observed only for branched $(Man)_5$. The mobility-selected tandem spectra validated the experimental mobility and dissociation data of individual precursor ions, demonstrating that IMS is a valuable tool to separate compounds with subtle structure

differences which can be difficult and time consuming for LC or which involves derivatization for GC,[67, 68] and is impossible with MS or MS^n alone.

To study the isomeric heterogeneity of product ions, as described in mode 3, mobility- and mass-selected pentasaccharide precursor ions were dissociated in the trap cell and the TWIMS was utilized to separate any remaining precursor and product ions. Figure 7 displays the overlaid traveling wave ion mobility spectra for product ions of *m/z* 509, 527, 671 and 689 generated from cellopentaose, maltopentaose and of branched $(Man)_5$. First, more than one mobility peak was frequently detected for specific product ions derived from one isomeric compound. For example, two mobility peaks were found for the *m/z* 527 product ion(s) derived from maltopentaose as shown in Figure 7b. More obviously, two partially or baseline separated isomeric mobility peaks were observed for all four product ions of cellopentaose (blue traces in Figures 7a–d). This suggests that multiple structural configurations exist for each specific product ion. This could be the result of structural differences at the free reducing end –OH included in the fragment ion, or could represent completely different fragmentation pathways giving rise to very different isomeric species. Either types of product ions may arise in different proportions from the corresponding multiple isomeric forms of reducing precursor ions. Second, by comparing the mobility distributions of single product ions derived from the three isomeric precursors, it was noticed that they had different drift times even though not fully resolved. This is reasonable and not unexpected. As these isomeric precursor ions had different stereochemistries and/or anomeric configurations, the product ions generated from them should be structurally unique, thus resulting in different mobilities. As shown in Figure 7a, *m/z* 509 of branched $(Man)_5$ drifted faster than *m/z* 509 from maltopentaose, and overlapped with one of the two mobility peaks of *m/z* 509 derived from cellopentaose. For product ions of *m/z* 671 and 689 displayed in Fig. 7c and d, maltopentaose and branched $(Man)_5$ showed similar mobilities and overlapped with the slower drifting mobility peak of cellopentaose. Another phenomenon worthy of note was that the mobility elution order of product ions can be similar or different from the mobility distribution orders of their corresponding precursor ions. For example, in Figure 7d, the *m/z* 689 product ion of cellopentaose drifted fastest, that of maltopentaose was of intermediate mobility, and that of branched $(Man)_5$ drifted slowest which matched with the relative orders of the mobilities of their precursor ions (Figure 5). However, Figure 7b demonstrated the opposite scenario where, for the product ion of *m/z* 527, branched $(Man)_5$ had smallest drift time as compared to maltopentaose and cellopentaose, while its precursor ion had the largest drift time as displayed in Figure 5. Again, this is not unexpected as isomeric product ions may have product ions that need not correlate in the magnitude of their overall cross-sectional areas with any relationship between their isomeric precursor ions. In all, the mobility of an oligosaccharide depends on its overall structural configuration when coordinated to a Na^+ ion. In addition, due to the limited resolving power of TWIMS, isomeric ions with completely different structures could happen to coincidentally co-migrate, thus each independent peak may represent more than one ion structure. Overall, the data presented herein provides direct evidence for the isomeric heterogeneity of carbohydrate product ions for the first time. (The MS/MS spectra and TWIMS spectra of product ions acquired from individual standards are included in Figures S-5 and S-6 in supporting information).

Conclusion

A lab built atmospheric pressure dual gate IMS was successfully coupled to a Synapt G2 HDMS instrument, resulting in a hybrid IMMS-IMMS instrument. Isomeric mixtures of oligosaccharides including disaccharide-alditols, trisaccharides and pentasaccharides were differentiated in the positive mode as sodiated adducts. The mobility elution order of compounds was the same for DTIMS and TWIMS, but the higher resolving power of

DTIMS enabled better separation among isomers. For mobility-selected fragmentation patterns, isomers having subtle structural differences generated identical product ions with different relative intensities; unique product ions were observed for isomers having larger structural variations. The concepts of carbohydrate isomer separation and mobility-selected fragmentation were demonstrated previously,[54–57] however, the addition of TWIMS after the collision cell in this hybrid instrument offers a method to evaluate the isomeric heterogeneity of product ions for mass- and mobility-selected precursor ions. Different mobilities were observed for product ions having identical *m/z* values. This information is valuable as it establishes a direct precursor-product relationship between mobility-selected precursor ions and specific sets of product ions having unique mobilities in addition to specific *m/z* values. These data should serve as further useful information to uniquely identify individual carbohydrate isomers, allowing unambiguous assignments of different oligosaccharide isomers within mixtures. This hybrid instrument demonstrated here can provide valuable information not obtainable with typical CID of *m/z*-selected precursor ions with added value for structural characterization of isomeric carbohydrates.

Additionally, interfacing a linear drift tube IMS to the Synapt G2 directly enables simple, accurate and straightforward calibration[48] of the traveling wave mobility cell for future studies. Furthermore, the concept of an IMMS-IMMS system demonstrated in this study could be extended to other types of ion mobility devices, such as differential mobility spectrometry,[69, 70] which can serve as a mobility filter and may be capable of providing additional advantages. The development of alternative IMS and Synapt G2 combinations is possible, which would promote greater in depth studies of gas phase ions than are not possible with current instruments.

Supplementary Material

Refer to Web version on PubMed Central for supplementary material.

Acknowledgments

This work was supported in part by the National Institutes of Health with Grant # 5R33RR020046. The authors acknowledge Eric Davis (Herbert H. Hill lab, Washington State University) for the software update of dual gate DTIMS system. Kevin Giles and Iain Lloyd (Waters, Manchester) are thanked for help in defeating the ion source interlock on the Synapt G2.

References

1. Cohen MJ, Karasek FW. J. Chromatogr. Sci. 1970; 8:330–337.
2. Griffin GW, Dzidic I, Carroll DI, Stillwell RN, Horning EC. Anal. Chem. 1973; 45:1204–1209.
3. Carroll DI, Dzidic I, Stillwell RN, Horning EC. Anal. Chem. 1975; 47:1956–1959.
4. Karasek FW, Kim SH, Hill HH Jr. Anal. Chem. 1976; 48:1133–1137.
5. Spangler GE, Lawless PA. Anal. Chem. 1978; 50:884–892.
6. Fetterolf DD, Clark TD. J. Forensic Sci. 1993; 38:28–39.
7. Ewing RG, Miller CJ. Field Anal. Chem. Technol. 2001; 5:215–221.
8. Tam M, Hill HH Jr. Anal. Chem. 2004; 76:2741–2747. [PubMed: 15144183]
9. Steiner WE, Clowers BH, Fuhrer , Gonin M, Matz LM, Siems WF, Schultz AJ, Hill HH Jr. Rapid Commun. Mass Spectrom. 2001; 15:2221–2226. [PubMed: 11746889]
10. Kanu AB, Hill HH Jr. Talanta. 2007; 73:692–699. [PubMed: 19073090]
11. Dwivedi P, Hill HH Jr. Int. J. Ion Mobil. Spec. 2008; 11:61–69.
12. Steiner WE, Clowers BH, Matz LM, Siems WF, Hill HH Jr. Anal. Chem. 2002; 74(17):4343–4352. [PubMed: 12236341]

13. Steiner WE, Clowers BH, Haigh PE, Hill HH Jr. Anal. Chem. 2003; 75:6068–6076. [PubMed: 14615983]
14. Steiner WE, Klopsch SJ, English WA, Hill H,H Jr. Anal. Chem. 2005; 77:4792–4799. [PubMed: 16053290]
15. Hoaglund-Hyzer CS, Lee YJ, Counterman AE, Clemmer DE. Anal. Chem. 2002; 74:992–1006. [PubMed: 11925002]
16. Wu C, Siems WF, Hill HH Jr. Anal. Chem. 2000; 72:391–395. [PubMed: 10658335]
17. Clemmer DE, Hudgins RR, Jarrold MF. J. Am. Chem. Soc. 1995; 117:10141–10142.
18. Eiceman, GA.; Karpas, Z. Ion Mobility Spectrometry. 2nd ed.. CRC Press, Taylor and Francis Group; Boca Raton, FL: 2005.
19. Eiceman GA. Trends Anal. Chem. 2002; 21:259–275.
20. Helden GV, Wyttenback T, Bowers MT. Int. J. Mass Spectrom. 1995; 146/147:349–364.
21. Hoaglund CS, Valentine SJ, Clemmer DE. Anal. Chem. 1997; 69:4156–4161.
22. Wu C, Siems WF, Asbury GR, Hill HH Jr. Anal. Chem. 1998; 70:4929–4938. [PubMed: 21644676]
23. Clowers BH, Hill HH Jr. Anal. Chem. 2005; 77:5877–5885. [PubMed: 16159117]
24. Kanu AB, Dwivedi P, Tam M, Matz L, Hill HH Jr. J. Mass Spectrom. 2008; 43:1–22. [PubMed: 18200615]
25. Li H, Giles K, Bendiak B, Kaplan K, Siems WF, Hill HH Jr. Anal. Chem. 2012; 84:3231–3239. [PubMed: 22339760]
26. Dwivedi P, Schultzb AJ, Hill HH Jr. Int. J. Mass Spectrom. 2010; 298:78–90. [PubMed: 21113320]
27. Wu C, Klasmeier J, Hill HH Jr. Rapid Commun. Mass Spectrom. 1999; 13:1138–1142. Jr. [PubMed: 10390859]
28. Fenn LS, Mclean JA. Anal. Bioanal. Chem. 2008; 391:905–909. [PubMed: 18320175]
29. Fenn LS, Kliman M, Mahsut A, Zhao SR, Mclean JA. Anal. Bioanal. Chem. 2009; 394:235–244. [PubMed: 19247641]
30. Kaplan K, Dwivedi P, Davidson S, Yang Q, Tso P, Siems W, Hill HH Jr. Anal. Chem. 2009; 81:7944–7953. [PubMed: 19788315]
31. Plasencia MD, Isailovic D, Merenbloom SI, Mechref Y, Clemmer DE. J. Am. Soc. Mass Spectrom. 2008; 19:1706–1715. [PubMed: 18760624]
32. Dwivedi P, Wu P, Klopsch SJ, Puzon GJ, Xun L, Hill HH Jr. Metabolomics. 2008; 4:63–80.
33. Dwivedi P, Puzon G, Tam M, Langlais , Jackson S, Kaplan K, Siems F, Schultz J, Xun L, Woods A, Hill HH Jr. J. Mass. Spectrom. 2010; 45:1383–1393. [PubMed: 20967735]
34. Isailovic D, Kurulugama RT, Plasencia MD, Stokes ST, Kyselova Z, Goldman R, Mechref Y, Novotny MV, Clemmer DE. J. Proteome Res. 2008; 7:1109–1117. [PubMed: 18237112]
35. Jin L, Barran PE, Deakin JA, Lyon M, Uhrin D. Phys. Chem. Chem. Phys. 2005; 7:3464–3471. [PubMed: 16273147]
36. Valentine SJ, Plasencia MD, Liu XY, Krishnan M, Naylor S, Udseth HR, Smith RD, Clemmer DE. J. Proteome Res. 2006; 5:2977–2984. [PubMed: 17081049]
37. McLean JA, Ruotolo BT, Gillig KJ, Russell DH. Int. J. Mass Spectrom. 2005; 240:301–315.
38. Purves RW, Barnett DA, Ells B, Guevremont R. J. Am. Soc. Mass Spectrom. 2001; 12:894–901. [PubMed: 11506222]
39. Giles K, Pringle SD, Worthington KR, Little D, Wildgoose JL, Bateman RH. Rapid Commun. Mass Spetrom. 2004; 18:2401–2414.
40. Pringle SD, Giles K, Wildgoose JL, Williams JP, Slade SE, Thalassinos K, Bateman RH, Bowers MT, Scrivens JH. Int. J. Mass Spectrom. 2007; 261:1–12.
41. Shvartsburg AA, Smith RD. Anal. Chem. 2008; 80:9689–9699. [PubMed: 18986171]
42. Giles K, Williams JP, Campuzano I. Rapid Commun. Mass Spetrom. 2011; 25:1559–1566.
43. Zhong Y, Hyung SJ, Ruotolo BT. Analyst. 2011; 136:3534–3541. [PubMed: 21445388]
44. Eckers C, Laures AM-F, Giles K, Major H, Pringle S. Rapid Commun. Mass Spectrom. 2007; 21:1255–1263. [PubMed: 17340559]

45. Rand KD, Pringle SD, Murphy JP III, Fadgen KE, Brown J, Engen JR. Anal. Chem. 2009; 81:10019–10028. [PubMed: 19921790]
46. Ridenour WB, Kliman M, Mclean JA, Caprioli RM. Anal. Chem. 2010; 82:1881–1889. [PubMed: 20146447]
47. Yamagaki T, Sato A. J. Mass. Spectrom. 2009; 44:1509–1517. [PubMed: 19753613]
48. Bush MF, Hall Z, Giles K, Hoyes J, Robinson CV, Ruotolo BT. Anal. Chem. 2010; 82:9557–9565. [PubMed: 20979392]
49. Williams JP, Grabenauer M, Holland RJ, Carpenter CJ, Wormald MR, Giles K, Harvey DJ, Bateman RH, Scrivens JH, Bowers MT. Int. J. Mass Spectrom. 2010; 298:119–127.
50. Martensson S, Levery SB, Fang TT, Bendiak B. Eur. J. Biochem. 1998; 258:603–622. [PubMed: 9874229]
51. Fang TT, Bendiak B. J. Am. Chem. Soc. 2007; 129:9721–9736. [PubMed: 17629269]
52. Mahal LK. Anti-Cancer Agents Med. Chem. 2008; 8:37–51.
53. Dwivedi P, Bendiak B, Clowers BH, Hill HH Jr. J. Am. Soc. Mass Spectrom. 2007; 18:1163–1175. [PubMed: 17532226]
54. Clowers BH, Dwivedi P, Steiner WE, Hill HH Jr. Bendiak B. J. Am. Soc. Mass Spectrom. 2005; 16:660–669. [PubMed: 15862767]
55. Zhu M, Bendiak B, Clowers B, Hill HH Jr. Anal. Bioanal.Chem. 2009; 394:1853–1867. [PubMed: 19562326]
56. Clowers BH, Hill HH Jr. J. Mass Spectrom. 2006; 41:339–351. [PubMed: 16498610]
57. Zucker SM, Lee S, Webber N, Valentine SJ, Reilly JP, Clemmer DE. J. Am. Soc. Mass Spectrom. 2011; 22:1477–1485. [PubMed: 21953250]
58. Liu Y, Clemmer DE. Anal. Chem. 1997; 69:2504–2509. [PubMed: 21639386]
59. Cerda BA, Wesdemiotis C. Int. J. Mass Spectrom. 1999; 189:189–204.
60. Lee S, Wyttenbach T, Bowers MT. Int. J. Mass Spectrom. 1997; 167/168:605–614.
61. Domon B, Costello CE. Glycoconjugate J. 1988; 5:397–409.
62. Hoaglund CS, Valentine SJ, Clemmer DE. Anal. Chem. 1997; 69:4156–4161.
63. Bendiak B, Salyan ME, Pantoja M. J. Org. Chem. 1995; 60:8245–8256.
64. Poulter L, Burlingame AL. Methods Enzymol. 1990; 193:661–689. [PubMed: 2074841]
65. Hofmeister GE, Zhou Z, Leary JA. J. Am Chem. Soc. 1991; 113:5964–5970.
66. Brown DJ, Stefan SE, Berden G, Steill JD, Oomens J, Eyler JR, Bendiak B. Carbohydr. Res. 2011; 346:2460–2481.
67. Karlsson H, Carlstedt I, Hansson GC. Anal. Biochem. 1989; 182:438–446. [PubMed: 2610361]
68. Thomsson KA, Hinojosa-Kurtzberg M, Axelsson KA, Domino SE, Lowe JB, Gendler SJ, Hansson GC. Biochem. J. 2002; 367:609–616. [PubMed: 12164788]
69. Eiceman GA, Krylov EV, Tadjikov B, Ewing RG, Nazarov EG, Miller RA. Analyst. 2004; 129:297–304. [PubMed: 15042159]
70. Krylov EV, Coy SL, Nazarov EG. Int. J. Mass Spectrom. 2009; 279:119–125.

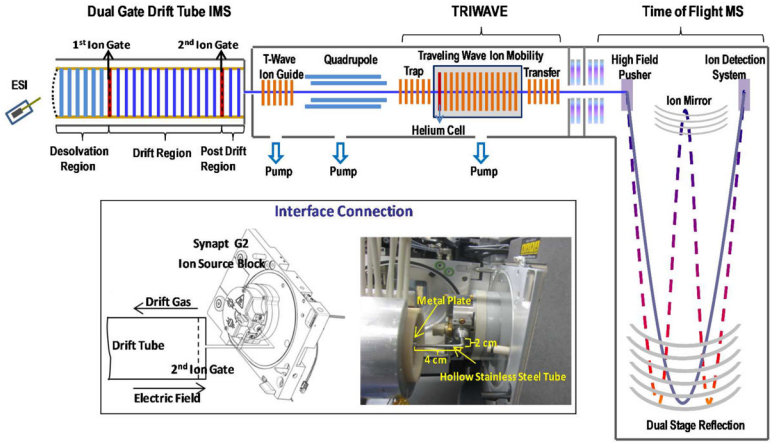

Figure 1.

Schematics of the instrument, showing the electrospray ionization (ESI) source, the ambient pressure, dual gate ion mobility drift tube, and the Synapt G2 high definition mass spectrometry unit that includes a quadrupole, a traveling wave ion mobility region and a dual stage reflectron time-of-flight mass spectrometer. The inserted window shows the detailed interface connection.

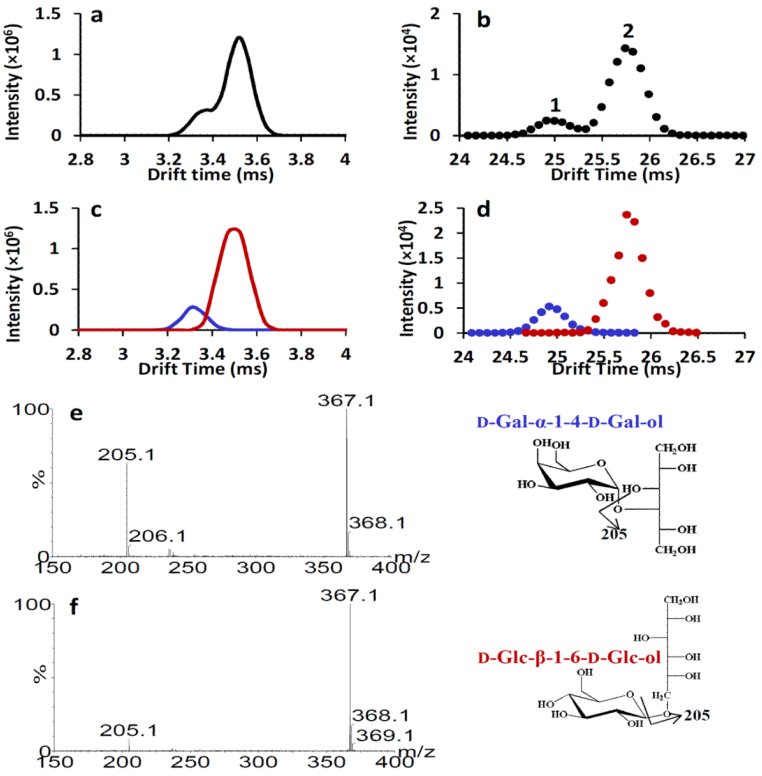

Figure 2.

(a) TWIMS separation of a disaccharide-alditol mixture (precursor *m/z* [M + Na^+] = 367. (b) DTIMS separation of the same disaccharide-alditol mixture. (c) Overlaid individual spectra of D-Gal-α-1-4-D-Gal-ol (blue) and D-Glc-β-1-6-D-Glc-ol (red) obtained on TWIMS. (d) Overlaid individual spectra of D-Gal-α-1-4-D-Gal-ol (blue) and D-Glc-β-1-6-D-Glc-ol (red) obtained on DTIMS. (e) Mobility selected MS/MS spectrum of mobility peak 1 (from panel b) using a 24.5–25.2 ms window on the dual gate DTIMS. The structure and fragmentation pathway for D-Gal-α-1-4-D-Gal-ol are shown on the right. (f) Mobility selected MS/MS spectrum of mobility peak 2 using a 25.5–26.5 ms window on the dual gate DTIMS. The structure and fragmentation pathway for D-Glc-β-1-6-D-Glc-ol are shown on the right. Note: (a) and (c) were obtained with the system operating in mode 1; (b) and (d) were collected using operation mode 2; (e) and (f) were acquired with mode 3 as described in the experimental section.

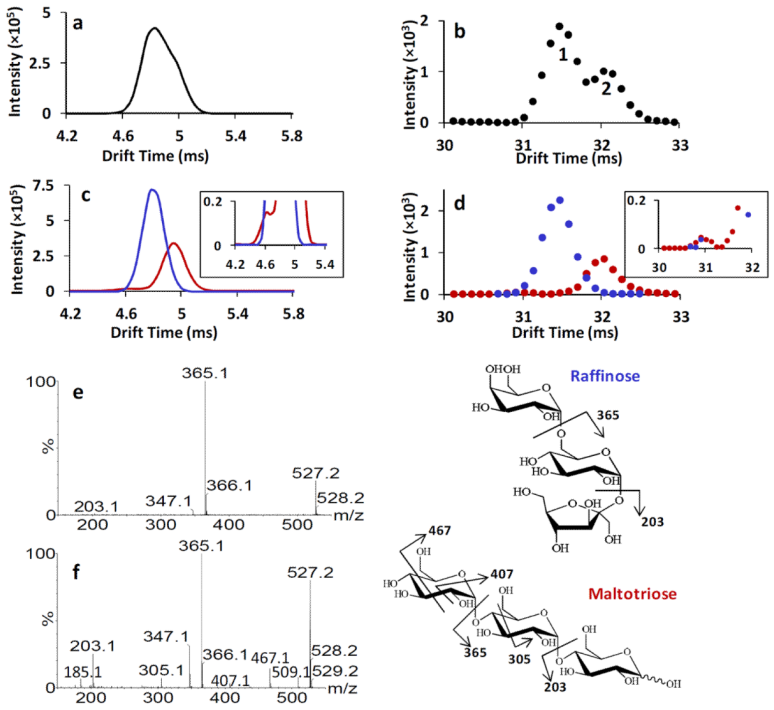

Figure 3.

(a) TWIMS separation of a trisaccharide mixture (precursor *m/z* [M + Na^+] = 527. (b) DTIMS separation of the same mixture. (c) Overlaid individual spectra of raffinose (blue) and maltotriose (red) obtained on TWIMS. (d) Overlaid individual spectra of raffinose (blue) and maltotriose (red) obtained on DTIMS. (e) Mobility selected MS/MS spectrum of mobility peak 1 using the drift time window of 31–31.5 ms on DTIMS (panel b). The structure and fragmentation pathway for raffinose are shown on the right. (f) Mobility selected MS/MS spectrum of mobility peak 2 using the drift time window of 32–32.5 ms on DTIMS (panel b). The structure and fragmentation pathway for maltotriose are shown on the right. Note: (a) and (c) were obtained with the system operating in mode 1; (b) and (d) were collected using mode 2; (e) and (f) were acquired with operation mode 3.

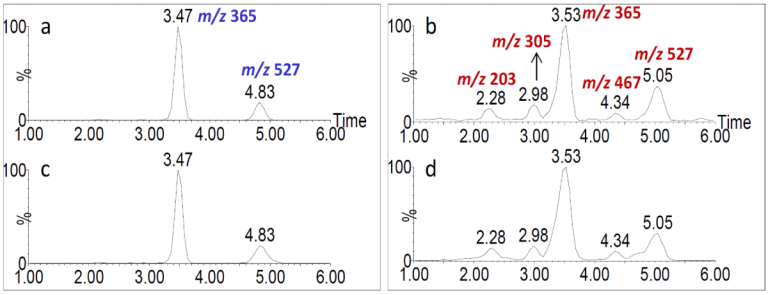

Figure 4.

(a) TWIMS separation of product ions derived from mobility selected peak 1 (raffinose) shown in Figure 3, panel b, fragmentation in panel e. (b) TWIMS separation of product ions for mobility selected peak 2 (maltotriose) shown in Figure 3, panel b, fragmentation in panel f. (c) TWIMS separation of raffinose and its product ions acquired from the standard run individually where the system was operated in mode 1. (d) TWIMS separation of maltotriose and its product ions acquired from the standard run individually (mode 1). The corresponding *m/z* values for the major resolved product ion mobility peaks were labeled in Figures 4a and 4b.

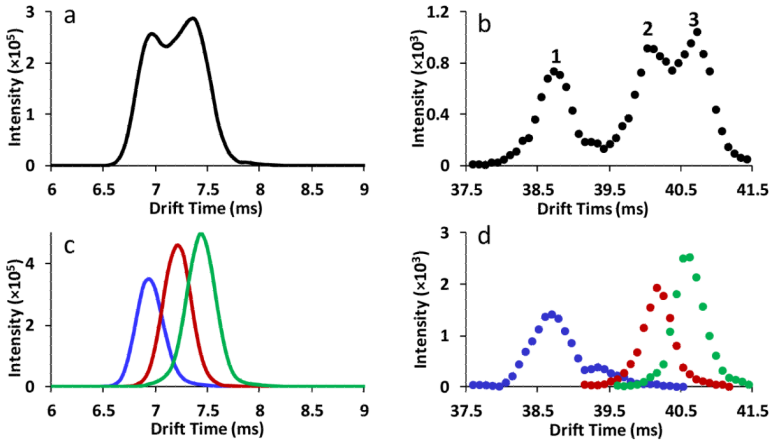

Figure 5.

(a) TWIMS separation of a pentasaccharide mixture (precursor *m/z* [M + Na^+] = 851). (b) DTIMS separation of the same pentasaccharide mixture. (c) Overlaid individual spectra of cellopentaose (blue), maltopentaose (red) and branched $(Man)_5$ (green) obtained on the TWIMS. (d) Overlaid individual spectra of cellopentaose (blue), maltopentaose (red) and branched $(Man)_5$ (green) obtained on the DTIMS. Note: (a) and (c) were collected with the system operating in mode 1 and (b) and (d) were obtained using operation mode 2 as explained in the experimental section.

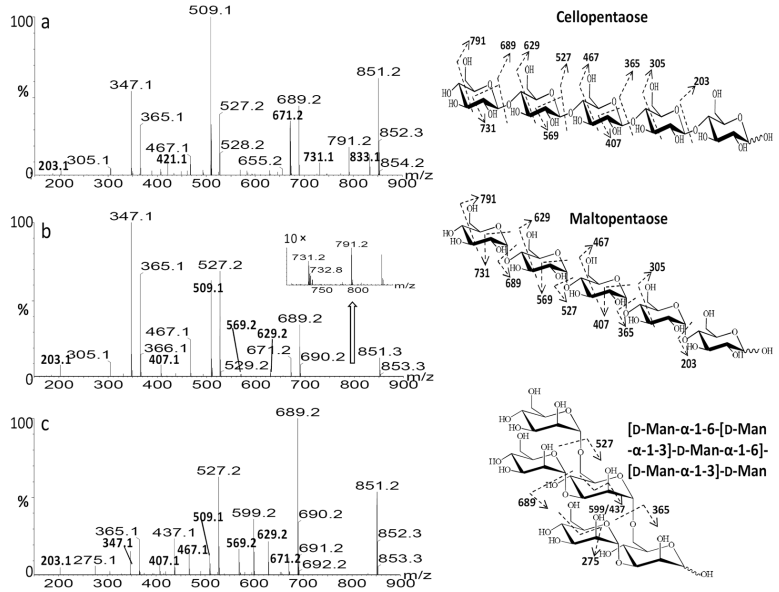

Figure 6.

Mobility-selected MS/MS spectra of pentasaccharides separated on the drift tube ion mobility region of the instrument. (a) Mobility-selected MS/MS spectrum of peak 1 (Figure 5b) using the drift time window of 38–38.7 ms on DTIMS. The structure and proposed fragmentation pathway of cellopentaose are shown on the right. (b) Mobility-selected MS/MS spectrum of peak 2 (Figure 5b) using the drift time window of 39.5–40.3 ms on DTIMS. The structure and fragmentation pathway of maltopentaose are shown on the right. and is not shown here. (c) Mobility-selected MS/MS spectrum for peak 3 (Figure 5b) using the drift time window of 40.6–41.5 ms on DTIMS. The structure and proposed fragmentation pathway of branched $(Man)_5$ are displayed on the right.

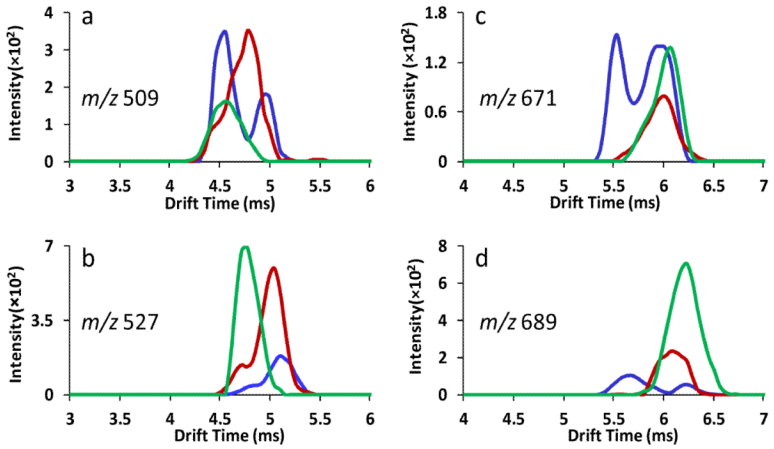

Figure 7.

Overlaid TWIMS separation of product ions derived from isomeric pentasaccharide precursor ions at *m/z* 851. (a) Overlaid TWIMS separation of product ion *m/z* 509 for cellopentaose (blue), maltopentaose (red) and branched $(Man)_5$ (green). (b) Overlaid TWIMS separation of product ion *m/z* 527 for cellopentaose (blue), maltopentaose (red) and branched $(Man)_5$ (green). (c) Overlaid TWIMS separation of product ion *m/z* 671 for cellopentaose (blue), maltopentaose (red) and branched $(Man)_5$ (green). (d) Overlaid TWIMS separation of product ion *m/z* 689 for cellopentaose (blue), maltopentaose (red) and branched $(Man)_5$ (green).